

# DEMoGen: Towards Decompositional Human Motion Generation with Energy-Based Diffusion Models

Jianrong Zhang<sup>1</sup>, Hehe Fan<sup>2,†</sup>, Yi Yang<sup>2</sup>

<sup>†</sup>Corresponding author

<sup>1</sup>ReLER, AAI, University of Technology Sydney    <sup>2</sup>CCAI, Zhejiang University

<https://jiro-zhang.github.io/DeMoGen/>

## Abstract

*Human motions are compositional: complex behaviors can be described as combinations of simpler primitives. However, existing approaches primarily focus on forward modeling, e.g., learning holistic mappings from text to motion or composing a complex motion from a set of motion concepts. In this paper, we consider the inverse perspective: decomposing a holistic motion into semantically meaningful sub-components. We propose DEMoGen, a compositional training paradigm for decompositional learning that employs an energy-based diffusion model. This energy formulation directly captures the composed distribution of multiple motion concepts, enabling the model to discover them without relying on ground-truth motions for individual concepts. Within this paradigm, we introduce three training variants to encourage a decompositional understanding of motion: ① DEMoGen-EXP explicitly trains on decomposed text prompts; ② DEMoGen-OSS performs orthogonal self-supervised decomposition; ③ DEMoGen-SC enforces semantic consistency between original and decomposed text embeddings. These variants enable our approach to disentangle reusable motion primitives from complex motion sequences. We also demonstrate that the decomposed motion concepts can be flexibly recombined to generate diverse and novel motions, generalizing beyond the training distribution. Additionally, we construct a text-decomposed dataset to support compositional training, serving as an extended resource to facilitate text-to-motion generation and motion composition.*

## 1. Introduction

Humans are inherently capable of decomposing complex motions into a set of simpler motion primitives. For example, we can easily interpret a motion “walking in a zigzag pattern while waving left hand” as a composition of two motion concepts, *i.e.*, “walking in a zigzag pattern” and “waving

left hand”. Such decompositional understanding allows humans to perform unusual motions by recombining known primitives, without extensive practice or prior exposure.

In the past few years, text-to-motion generation has achieved remarkable progress, mainly attributed to the availability of large-scale motion datasets and advances in powerful generative models. Most state-of-the-art approaches focus on producing high-fidelity motions that are semantically aligned with a single textual description [20, 44, 61, 66, 70, 72, 73, 78]. In parallel, several works have begun to explore compositional motion generation [2, 3, 31, 46, 53, 64]. They leverage pre-trained diffusion models through spatial editing and temporal concatenation for fine-grained control and generating long-duration motions, respectively. More recently, EnergyMoGen [71] presents two spectrums of energy-based models and achieves motion composition through energy aggregation. The approach also introduces additional logical operators, *i.e.*, negation and combination of conjunction and negation, to enable more diverse forms of composition.

Despite these advances, existing approaches treat motion as a holistic sequence, without capturing its structured composition of motion concepts. This lack of decompositional understanding limits their ability to infer and recombine concepts like humans do. A natural question thus arises: *how can we endow generative models with a human-like ability to disentangle the underlying motion concepts?*

As a response to this question, we propose DEMoGen, a compositional training paradigm that learns to decompose motions into a set of semantically interpretable motion concepts under compositional supervision. Building upon the intrinsic relationship between diffusion models [23, 52, 57] and Energy-Based Models(EBMs) [9, 33, 77], we represent each motion concept as an energy score. Unlike previous methods that typically learn a one-to-one mapping between text and motion, our approach models the composed energy distribution of multiple motion concepts during training. This design enforces concept-level factorization, which naturally enables motion decomposition at inference, and

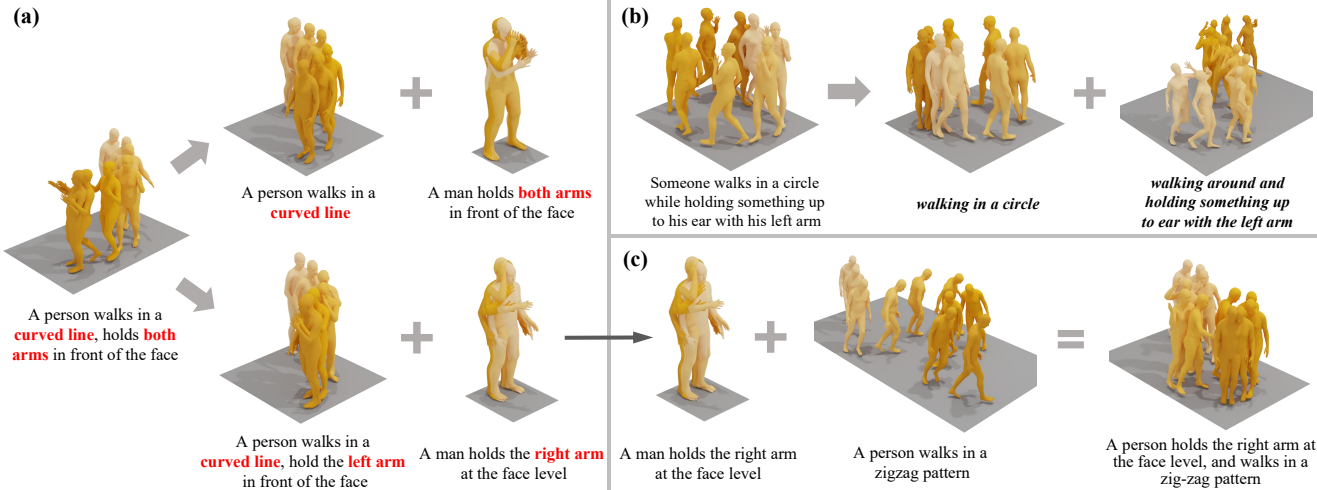


Figure 1. **Decompositional motion generation.** (a) Our approach is able to decompose a holistic motion into multiple motion concepts with DEMOGEN-EXP. This process is explicitly guided by decompositional textual descriptions, yielding diverse decomposition outcomes when varying the text cues. (b) Our approach also supports unguided decomposition using DEMOGEN-OSS and DEMOGEN-SC, where the model infers motion concepts without explicit decompositional text. We manually caption the inferred concepts in italic for easy understanding. (c) The decomposed motion primitives can be recombined to synthesize diverse and novel motions.

further supports flexible concepts recombination for compositional motion generation (Figure 1(a), (b), (c)).

More specifically, we explore three variants of DEMOGEN, reflecting varying degrees of compositional supervision: ① DEMOGEN-EXP introduces *explicit supervision* by training on decomposed text prompts, where each motion concept is conditioned on its corresponding textual description. Such explicit pairing enforces clear semantic boundaries for precise and diverse concept factorization (Figure 1(a)); ② DEMOGEN-OSS operates under *orthogonal self-supervision*. We partition the holistic text embedding into multiple segments and directly train the model on these segments. An orthogonality loss is applied to encourage disentanglement without additional explicit constraints, enabling unguided decomposition and improving motion diversity. ③ DEMOGEN-SC leverages *semantic consistency supervision* by aligning each partitioned text embedding segment with the corresponding decomposed text embeddings. This also enables unguided decomposition at inference (Figure 1(b)).

To support explicit and semantic consistency supervisions, we construct a DecompML dataset, an extension of the widely used HumanML3D [18] with *decompositional* text annotations. We break down original holistic motion descriptions into semantically interpretable concepts using large language models. Importantly, our dataset can also serve as a benchmark for compositional motion generation, promoting future research in this field.

DEMOGEN is a unified training paradigm that simultaneously facilitates text-to-motion generation, multi-concept generation, as well as decompositional and compositional (including concept recombination) motion generation. With

its general formulation, our approach is compatible with both latent and semantic-aware EMBs [71] and can seamlessly integrate with mainstream diffusion-based methods. Extensive experiments demonstrate the effectiveness of DEMOGEN, showing robust improvements on both text-to-motion and motion composition benchmarks *i.e.*, HumanML3D [18] and MTT [46]. In particular, we observe significant improvements in the compositional and multi-concept motion generation tasks. Moreover, by pairing decomposed motions with their corresponding text concepts, DecompML can serve as an augmented motion-language dataset, which further benefits text-to-motion generation.

## 2. Related Works

**Text-to-Motion Generation.** Text-to-motion generation, which seeks to generate temporally coherent and physically plausible motion sequences from text instructions, has attracted increasing attention in recent years. Early studies in this area are typically based on autoencoder architectures [1, 15, 60]. They establish cross-modal correspondences by projecting text and motion into a shared latent representation, but suffer from deterministic mappings that limit motion diversity and realism. Researchers [18, 43–45] adopt probabilistic frameworks, *i.e.*, Variational Autoencoders (VAEs), which shift the focus from fixed encodings to distribution-based modeling, allowing diverse motion generation through sampling. Recent works introduce both autoregressive [19, 28, 39, 70, 75, 78] and non-autoregressive [20, 48] strategies inspired by natural language [4] and vision tasks [5], where the motion is represented as a sequence of discrete tokens via Vector Quantized-Variational Autoencoders (VQ-VAEs). For

example, T2M-GPT [70] adopts a GPT-like architecture, while MoMask [20] applies masked token prediction to generate motion from text prompts.

In parallel, diffusion models have emerged as a powerful alternative for motion synthesis. These models leverage iterative refinement to capture complex spatial-temporal dynamics. MotionDiffuse [72] and MDM [61] first show the feasibility of diffusion on text-to-motion generation. This line of research [7, 16, 21, 29, 51, 62, 65, 67–69, 73, 74, 79] applies diffusion directly to raw motion representations such as joint positions and rotations. Several works [13, 32, 38, 66] continue to investigate latent diffusion models [52]. MLD [66] is a representative motion latent diffusion model, and subsequent works [13, 32, 38] introduce architectural improvements, including GNN-based VAEs [24] and the Mamba framework [17, 76].

In contrast to these methods that learn a holistic text-to-motion mapping, we focus on a decompositional understanding of motion using an energy-based diffusion model. We demonstrate how a complex motion can be decomposed into a set of semantically interpretable motion concepts, and further show that these concepts can be flexibly recomposed to synthesize novel motions unseen during training.

**Compositional and Decompositional Generation.** Compositional and decompositional generation play a crucial role in achieving controllability and interpretability in generative modeling, and have been well explored in the image domain. Some compositional image generation approaches incorporate additional training strategies, such as contrastive learning [6, 34] and classifier guidance [14, 55]. Another line of work achieves compositional control at inference by modifying attention maps [12, 26, 27, 41] or composing the distributions of pre-trained generative models [8–11, 35, 36]. As for the decompositional generation, previous studies [22, 42, 49, 54, 56] aim to disentangle desired factor by operating in the latent space. Recently, inspired by EBMs, Liu *et al.* [37] leveraged pre-trained diffusion models to discover diverse visual concepts (*e.g.*, image class and style). Su *et al.* [59] focused on compositional concept decomposition, enabling both global and local concept factorization from a given image. In the compositional motion generation domain [2, 3, 47], most diffusion-based solutions [30, 53, 64] incorporate spatial and temporal control into the denoising process based on MDM [61] architecture. EnergyMoGen [71] formulates the denoising network and cross-attention as energy functions and combines their energy distributions in the latent space.

In this paper, we propose a compositional training paradigm for motion decomposition. We investigate three supervision regimes, ranging from explicit supervision to a fully self-supervised setting. By leveraging this paradigm, our approach seamlessly supports text-to-motion generation, motion composition, and motion decomposition

within a single model.

### 3. Method

In this section, we detail our approach, DEMOGEN. We first introduce background knowledge on interpreting diffusion models and cross-attention modules as parameterizing energy functions in Section 3.1. Next, we discuss how to use this interpretation to decompose a motion sequence into multiple composable motion concepts, which are then leveraged for compositional training in Section 3.2. We present three DEMOGEN variants in Section 3.3, reflecting different levels of compositional supervision. In Section 3.4, we introduce the DeCompML dataset. The overview of our approach is illustrated in Figure 2.

#### 3.1. Energy Perspectives of Diffusion Models

Denoising Diffusion Probabilistic Models [23] facilitate motion generation by progressively refining motion sequences corrupted with Gaussian noise. The model consists of a forward diffusion process and a reverse denoising process. The forward process is defined as a Markov chain that models the distribution  $q(\mathbf{x}_t | \mathbf{x}_{t-1}) = \mathcal{N}(\mathbf{x}_t; \sqrt{1 - \beta_t} \mathbf{x}_{t-1}, \beta_t I)$ , where the clean motion  $\mathbf{x}_0$  is gradually perturbed by Gaussian noise  $\epsilon \sim \mathcal{N}(0, I)$  over  $t$  steps. Then, a denoising network  $\epsilon_\theta$  is trained to predict the noise at each time step  $t$

$$\mathcal{L}_{\text{MSE}} = \|\epsilon - \epsilon_\theta(\mathbf{x}_t, t)\|^2. \quad (1)$$

Conversely, the reverse process seeks to recover the original motion by iteratively removing the added noise. Specifically, given a sample  $\mathbf{x}_T$  at noise level  $T$ , the motion can be denoised through

$$\mathbf{x}_{t-1} = \mathbf{x}_t - \epsilon_\theta(\mathbf{x}_t, t) + \mathcal{N}(0, \tilde{\beta}_t I), \quad (2)$$

where  $\tilde{\beta}$  denotes the posterior variance. Following prior efforts [9, 10, 36, 58, 63], the denoising network  $\epsilon_\theta(\mathbf{x}, t)$  can be interpreted as a score function  $\nabla_{\mathbf{x}} \log p(\mathbf{x})$ , which, in turn, establishes a correspondence with the energy function, *i.e.*,  $\epsilon_\theta(\mathbf{x}, t) \propto \nabla_{\mathbf{x}} E_\theta(\mathbf{x})$ , where  $p(\mathbf{x}) \sim e^{-E(\mathbf{x})}$ . Thus, with the step size  $\eta$ , Equation 2 is equivalent to

$$\mathbf{x}_{t-1} = \mathbf{x}_t - \eta \nabla_{\mathbf{x}} E_\theta(\mathbf{x}) + \mathcal{N}(0, \tilde{\beta}_t I). \quad (3)$$

EnergyMoGen [71] defines the preceding expression as a latent-aware EBM and also interprets cross-attention in the denoising network as a semantic-aware EBM. This formulation draws inspiration from modern Hopfield networks [25–27, 41, 50], which model associative patterns and contextual relationships within text embeddings. These energy-based interpretations motivate us to employ energy-based diffusion models (both latent- and semantic-aware) to represent a holistic motion using a set of energy functions, where each function captures a specific motion concept, collectively enabling a decompositional understanding of motion.

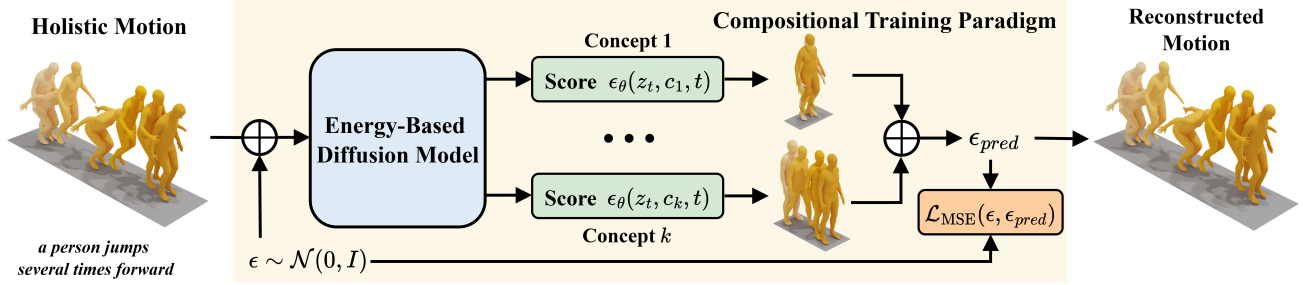


Figure 2. **Overview of our approach.** We propose DEMOGEN, a compositional training paradigm that facilitates decompositional motion generation via an energy-based diffusion model. We learn to decompose the holistic motion into  $K$  concepts. The energy functions of these concepts are aggregated to form the  $\epsilon_{pred}$ , which is subsequently trained to guide the denoising process. Energy aggregation can be achieved via a denoising network and a cross-attention, supporting either latent-aware or semantic-aware modeling 3.2. Furthermore, we investigate three variants (Section 3.3), which specify distinct strategies for learning or utilizing  $\{c_k\}_{k=1}^K$  within our approach.

#### Algorithm 1 Compositional Training Paradigm

```

1: Require: Frozen VAE encoder  $\mathcal{E}$ , denoising network  $\epsilon_\theta$ , number of training data  $N$ , learning rate  $\lambda$ 
2: for  $i = 1, \dots, N$  do
3:    $\mathbf{z}^i \leftarrow \mathcal{E}(\mathbf{x}^i)$ 
4:   // Initialize a Gaussian noise and a random time step
5:    $\epsilon \sim \mathcal{N}(0, 1)$ ,  $t \sim \mathcal{U}\{1, \dots, T\}$ 
6:    $\mathbf{z}_t^i = \sqrt{\bar{\alpha}_t} \mathbf{z}^i + \sqrt{1 - \bar{\alpha}_t} \epsilon$  //  $\bar{\alpha}_t = \prod_{i=1}^t (1 - \beta_i)$ 
7:   // Compute compositional denoising scores
8:   if mod is latent-aware then
9:      $\epsilon_{pred} \leftarrow \sum_{k=1}^K \epsilon_\theta(\mathbf{z}_t^i, \mathbf{c}_k, t)$ 
10:  end if
11:  if mod is semantic-aware then
12:    // Replace the cross-attention with DCA
13:     $\epsilon_{pred} \leftarrow \epsilon_\theta(\mathbf{z}_t^i, \mathbf{C}, t)$ 
14:  end if
15:   $\mathcal{L} = \text{MSE}(\epsilon, \epsilon_{pred})$  // Optimization goal
16:   $\theta \leftarrow \theta - \lambda \nabla_\theta \mathcal{L}$  // Update the model weight
17: end for

```

### 3.2. Decompositional Human Motion Generation with Energy-Based Diffusion Models

A well-performed text-to-motion model should not only synthesize text-aligned motions but also capture their underlying decompositional structure, *i.e.*, how a motion is composed of multiple primitives. To achieve this, our DEMOGEN reformulates the motion generation task from a decompositional perspective. We adopt a skeleton-aware latent diffusion architecture following [24]. Specifically, given a motion  $\mathbf{x} \in \mathbb{R}^{L \times d_m}$ , where  $L$  denotes the motion length and  $d_m$  is the feature dimensionality of each frame. We variationally encode the holistic motion  $\mathbf{x}$  into a latent representation  $\mathbf{z}$  using a motion encoder  $\mathcal{E}$ , and map it back to the motion space through a decoder  $\mathcal{D}$ .

Our key idea is to learn a set of energy functions to reconstruct a motion sequence using an energy-based diffusion model in a compositional manner. Driven by this in-

sight and the close connection between diffusion models and EBMs discussed in Section 3.1, we propose a compositional training paradigm. Concretely, at noise level  $t$ , the noisy latent  $\mathbf{z}_t$  is associated with a set of text embeddings  $\mathbf{C} = \{\mathbf{c}_k\}_{k=1}^K$ , each corresponding to a target motion concept, where  $K$  denotes the number of motion concepts decomposed from a holistic motion. Note that several strategies to obtain  $\{\mathbf{c}_k\}_{k=1}^K$  are detailed in Section 3.3.

We further investigate the accommodation of our training paradigm to the two spectra of EBMs [71], *i.e.*, latent-aware and semantic-aware, under the same principle with minimal modifications:

- *Latent-aware EBM* is realized by the denoising network, which is trained to capture the composed energy distribution across these  $K$  concepts using the objective:

$$\mathcal{L}_{\text{MSE}} = \|\epsilon - \sum_{k=1}^K \epsilon_\theta(\mathbf{z}_t, \mathbf{c}_k, t)\|^2. \quad (4)$$

- *Semantic-aware EBM* parameterizes the energy function via the cross-attention module. We propose a Decompositional Cross-Attention (DCA) mechanism that divides the attention computation into parallel branches. It performs  $K$  distinct attention operations with different key-value pairs and aggregates their outputs, formulated as

$$\text{DCA}(\mathbf{z}_t, \mathbf{C}) = \sum_{k=1}^K \text{CA}(\mathbf{z}_t, \mathbf{c}_k), \quad (5)$$

where CA indicates the standard cross-attention. We then optimize the entire model using the general optimization goal  $\mathcal{L}_{\text{MSE}} = \|\epsilon - \epsilon_\theta(\mathbf{z}_t, \mathbf{C}, t)\|^2$ .

With these energy functions effectively reconstructed, we can directly extract the specific and desired motion concepts from the learned decompositional space and further operate over them, thereby achieving motion decomposition and concept recombination. Furthermore, this compositional training paradigm can also improve the text-to-motion generation. We provide the pseudocode for our approach in Algorithm 1. The pseudocodes for sampling are provided in Appendix A.

Methods	R-Precision $\uparrow$			FID $\downarrow$	MM-Dist $\downarrow$	Diversity $\rightarrow$	MModality $\uparrow$
	Top-1	Top-2	Top-3				
<b>Real motion</b>	0.511 $\pm$ .003	0.703 $\pm$ .003	0.797 $\pm$ .002	0.002 $\pm$ .000	2.974 $\pm$ .008	9.503 $\pm$ .065	-
MDM [61]	0.418 $\pm$ .005	0.604 $\pm$ .001	0.707 $\pm$ .004	0.489 $\pm$ .025	3.630 $\pm$ .023	<u>9.450</u> $\pm$ .066	<b>2.870</b> $\pm$ .111
MLD [66]	0.481 $\pm$ .003	0.673 $\pm$ .003	0.772 $\pm$ .002	0.473 $\pm$ .013	3.196 $\pm$ .010	9.724 $\pm$ .082	2.413 $\pm$ .079
ReMoDiffusion [73]	0.510 $\pm$ .005	0.698 $\pm$ .006	0.795 $\pm$ .004	0.103 $\pm$ .004	2.974 $\pm$ .016	9.018 $\pm$ .075	1.795 $\pm$ .043
FineMoGen [74]	0.504 $\pm$ .002	0.690 $\pm$ .002	0.784 $\pm$ .004	0.151 $\pm$ .008	2.998 $\pm$ .008	9.263 $\pm$ .094	<u>2.696</u> $\pm$ .079
EnergyMoGen [71]	0.523 $\pm$ .003	0.715 $\pm$ .002	0.815 $\pm$ .002	0.188 $\pm$ .006	2.915 $\pm$ .007	<b>9.488</b> $\pm$ .099	2.205 $\pm$ .041
SALAD [24]	0.581 $\pm$ .003	0.769 $\pm$ .003	0.857 $\pm$ .002	<b>0.076</b> $\pm$ .002	2.649 $\pm$ .009	9.696 $\pm$ .096	1.751 $\pm$ .062
<i>latent-aware</i>							
DEMOGEN-EXP	0.569 $\pm$ .004	0.760 $\pm$ .005	0.850 $\pm$ .004	<u>0.078</u> $\pm$ .003	2.708 $\pm$ .012	9.774 $\pm$ .099	1.944 $\pm$ .054
DEMOGEN-SC	0.565 $\pm$ .003	0.757 $\pm$ .004	0.846 $\pm$ .003	0.121 $\pm$ .005	2.739 $\pm$ .009	9.933 $\pm$ .131	1.785 $\pm$ .044
DEMOGEN-OSS	<b>0.588</b> $\pm$ .004	<b>0.778</b> $\pm$ .002	<u>0.861</u> $\pm$ .003	0.092 $\pm$ .003	<u>2.625</u> $\pm$ .007	9.779 $\pm$ .120	1.748 $\pm$ .059
<i>semantic-aware</i>							
DEMOGEN-EXP	0.586 $\pm$ .005	0.776 $\pm$ .003	<b>0.863</b> $\pm$ .002	0.116 $\pm$ .008	<b>2.623</b> $\pm$ .008	9.873 $\pm$ .057	1.785 $\pm$ .046
DEMOGEN-SC	0.565 $\pm$ .002	0.758 $\pm$ .003	0.846 $\pm$ .003	0.138 $\pm$ .005	2.727 $\pm$ .010	9.769 $\pm$ .158	1.763 $\pm$ .046
DEMOGEN-OSS	0.584 $\pm$ .002	0.774 $\pm$ .003	0.858 $\pm$ .001	0.104 $\pm$ .005	2.637 $\pm$ .014	9.877 $\pm$ .127	1.742 $\pm$ .102

Table 1. **Comparison with the state-of-the-art diffusion models on the test set of HumanML3D [18].** We quantitatively evaluate our approach across three variants under both latent-aware and semantic-aware settings. All metrics are obtained via a pretrained evaluation model from Guo *et al.* [18]. **Bold** and underlined denote the best and second-best results, respectively.

### 3.3. DEMOGEN Variants

To comprehensively study the proposed training paradigm, we present three variants that reflect different levels of compositional supervision. For convenience, we denote  $\mathbf{C}^P = \{\mathbf{c}_k^P\}_{k=1}^K$  as the set of predefined decomposed text embeddings from our DeCompML dataset (Section 3.4). We present extensive ablation studies of these three variants in the appendix.

**DEMOGEN-EXP** provides *explicit supervision* by indicating the correspondence between the holistic motion and its decomposed textual descriptions, where  $\mathbf{C} = \mathbf{C}^P$ . Relying solely on decomposed textual descriptions for training may lead to inaccurate text–motion mapping and limit the model’s performance. To address this issue, we propose a text mixing strategy, that is, in each training batch,  $\tau \times 100\%$  of the motion samples are trained with the original textual descriptions instead of the decomposed ones.

**DEMOGEN-OSS** is trained with *orthogonal self-supervision*. Specifically, given an original text embedding  $\mathbf{c} \in \mathbb{R}^{L_c \times d_c}$ , we partition it along the dimensional axis into  $K$  sub-embeddings  $\hat{\mathbf{C}} = \{\hat{\mathbf{c}}_k\}_{k=1}^K$ , each of size  $d_c/K$ . We feed  $\hat{\mathbf{C}}$  into a fully connected layer to produce  $\mathbf{C}$ . We promote orthogonality among the components in  $\mathbf{C}$  using an orthogonalization loss  $\mathcal{L}_{\text{Ortho}}$ , following [59]. Training proceeds in a fully self-supervised manner, without relying on any predefined text embeddings. The training objective can be written as  $\mathcal{L} = \mathcal{L}_{\text{MSE}} + \alpha_o \mathcal{L}_{\text{Ortho}}$ , where  $\alpha_o$  is the weight of the orthogonalization loss.

**DEMOGEN-SC** splits the original text embedding following the same procedure as DEMOGEN-OSS, but uses two-

layer transformers to obtain  $\mathbf{C}$ . We employ *semantic consistency supervision* by encouraging the consistency property between the partitioned and decomposed text embeddings, which is  $\mathcal{L}_{\text{SC}} = \mathcal{L}_1^{\text{smooth}}(\mathbf{C}^P, \mathbf{C})$ . Furthermore, we also use  $\mathcal{L}_{\text{Ortho}}$  to encourage disentanglement. Thus, the overall optimization goal is  $\mathcal{L} = \mathcal{L}_{\text{MSE}} + \alpha_{sc} \mathcal{L}_{\text{SC}} + \alpha_o \mathcal{L}_{\text{Ortho}}$ , with an additional weight hyper-parameter  $\alpha_{sc}$ .

During inference, DEMOGEN-OSS and DEMOGEN-SC operate without the need for predefined decompositional texts, thus enabling unguided motion concept discovery (Section 4.4). We further observe that DEMOGEN-OSS benefits the diversity for generating holistic motions (Section 4.5). In contrast, DEMOGEN-EXP leverages decompositional texts to achieve more accurate and diverse motion decomposition, while also exhibiting superior compositional generation performance (Section 4.4). It’s worth noting that DEMOGEN-EXP supports single textual input for the text-to-motion generation task by duplicating the text to satisfy the required decompositional conditioning.

### 3.4. DeCompML Dataset

To support explicit and semantic consistency supervisions in DEMOGEN-EXP and DEMOGEN-SC mentioned above, we relabel the HumanML3D [18] dataset. HumanML3D collects 14,616 motion sequences, each paired with 3–4 textual descriptions summarizing the entire motion. We relabel these texts by splitting each into two sentences, which respectively depict different decompositional motion concepts within the holistic sequence. For example, a description such as “*someone runs forward, turns around, and then walks backward*” is extended into “*someone runs forward*

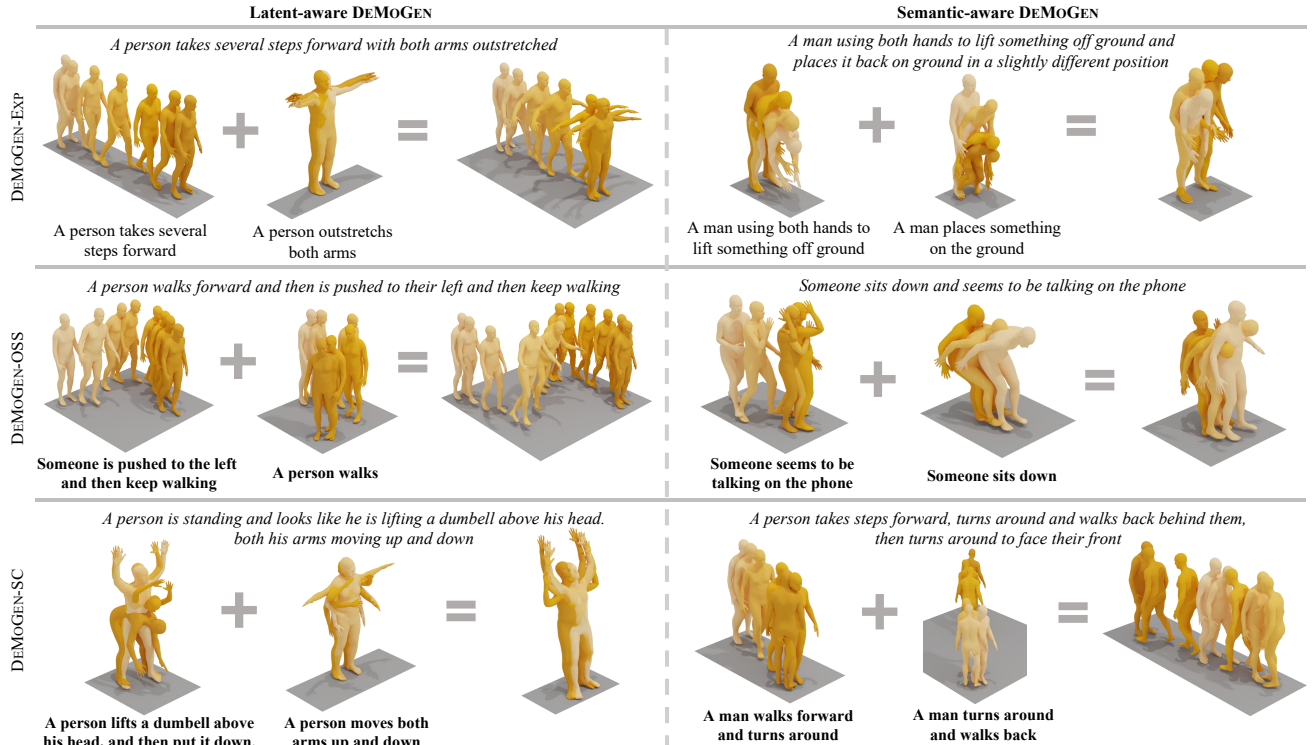


Figure 3. **Text-to-motion generation with decompositional understanding.** Given a complete textual description (in italics above the result), our approach first infers the motion concepts and further composes them to synthesize the holistic motion that matches the text. Notably, DEMOGEN-OSS and DEMOGEN-SC discover motion concepts without the aid of decomposed text. However, for clarity, we manually annotate each concept in **bold**. More visual results can be found on the [project page](#).

and turns around” and “someone walks backward”. This process is fully automated by prompting a large language model (*i.e.*, GPT-4.1 [40]) with carefully crafted instructions, constraints, *etc.* Considering that HumanML3D [18] already applies data augmentation strategies such as mirroring, our DeCompML dataset ultimately comprises 87,384 decomposed text groups (each containing two sentences, 174,768 in total). This dataset can serve as a new benchmark for compositional motion generation (Section 4.4).

With the relabeled textual descriptions, we sample decomposed motions in the HumanML3D training set via the learned DEMOGEN-EXP, and select 15,000 high-quality motion sequences as extended motion data. We demonstrate that jointly training on both the HumanML3D and the 15,000 decomposed motion-text pairs from DeCompML can improve text-to-motion generation (Section 4.5).

We provide the designed prompt, statistics of DeCompML, and ablative experiments on the number of textual splits in the appendix.

## 4. Experiments

In this section, we evaluate our approach across four tasks: text-to-motion generation (Section 4.3), decompositional and compositional motion generation (Section 4.4), as well

as multi-concept motion generation (Section 4.4). Analysis and discussion are provided in Section 4.5. More detailed information on datasets and evaluation metrics can be found in the appendix.

### 4.1. Datasets and Evaluation Metrics

**Datasets.** We conduct experiments on several benchmark datasets across different tasks. HumanML3D [18] and our DeCompML collectively support text-to-motion generation and decompositional motion generation by providing both holistic and decomposed motion-text pairs. To examine our approach under complex scenarios involving multiple motion concepts, we adopt the MTT [46] dataset for multi-concept generation and motion composition. Notably, the decomposed annotations of DeCompML also make it a suitable benchmark for motion composition tasks.

**Evaluation Metrics.** To evaluate the performance of our approach, we report R-Precision, MM-Dist, FID, Diversity, and MModality for text-to-motion generation following Guo *et al.* [18]. We employ the same metrics as text-to-motion for motion composition on DeCompML. On MTT [46], R-Precision, TMR-Score, FID, and transition distance are used as quantitative metrics for both compositional and multi-concept generation.

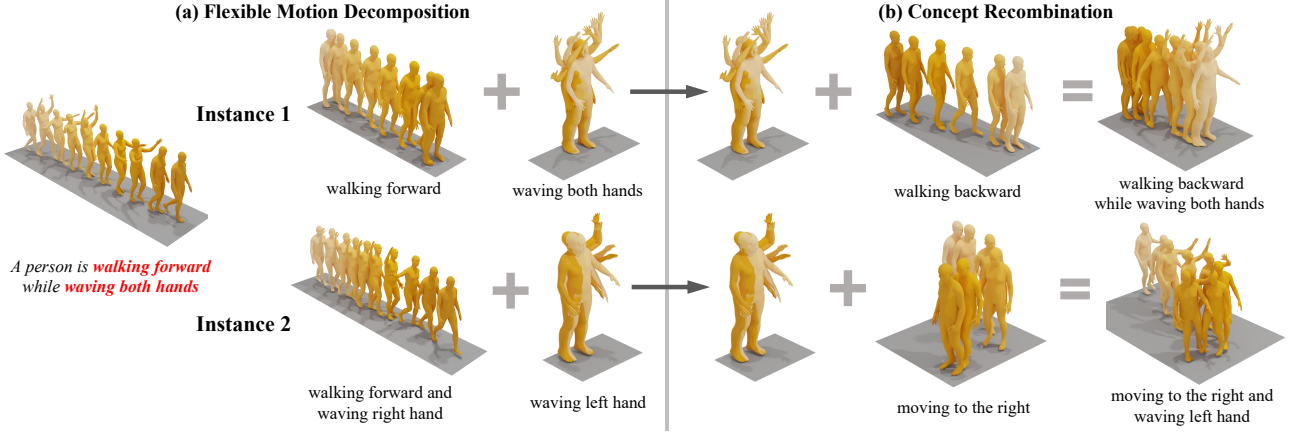


Figure 4. **Motion decomposition and recombination.** We demonstrate that our method can infer diverse motion concepts from a complex motion sequence, conditioned on different decompositional text prompts. Our approach also exhibits the ability to recombine the inferred concepts with others to generate novel motions.

Methods	R-Precision		TMR-Score ↑		FID ↓	Transition distance ↓
	R@1 ↑	R@3 ↑	M2T	M2M		
Multi-concept motion generation (single text)						
MotionDiffuse [72]	10.9	21.3	0.558	0.546	0.621	1.9
MDM [61]	9.5	19.7	0.556	0.549	0.666	2.5
ReModiffuse [73]	7.4	18.3	0.531	0.534	0.699	3.3
FineMoGen [74]	5.4	11.7	0.504	0.533	0.948	9.4
MLD [66]	10.5	22.3	0.559	0.552	0.685	2.4
EMG [71]	12.7	25.4	0.570	0.562	0.592	2.7
EMG+AGD [71]	14.0	26.3	0.570	0.560	0.587	2.7
DEMOGEN-SC <sup>†</sup>	14.3	29.7	0.578	0.568	0.585	2.7
DEMOGEN-OSS <sup>†</sup>	14.9	29.5	0.584	0.574	0.580	2.6
Compositional motion generation (multiple texts)						
EMG+SEF [71]	15.9	28.0	0.591	0.567	0.604	1.6
DEMOGEN-EXP <sup>†</sup>	16.2	31.9	0.597	0.570	0.621	1.6

Table 2. **Quantitative comparison on MTT [46].** The metrics are computed following STMC [46] and EnergyMoGen (EMG) [71]. <sup>†</sup> indicates the latent-aware setting. The results of the semantic-aware model are provided in the appendix.

## 4.2. Implementation Details

We use the VAE initialized with pretrained weights from [24]. We train the latent-aware and semantic-aware DEMOGEN using the AdamW optimizer with a batch size of 64 for 500 epochs. The initial learning rate is set to 2e-4 and decayed to 2e-5 after 50K iterations. We set  $K=2$  to model each holistic motion with two motion concepts, and following [59], we compute the final energy distribution by averaging  $K$  energy scores. For all three variants of DEMOGEN, the text replacement rate  $\tau$  is set to  $0.7 \times 100\%$  and  $\alpha_{sc}$  is set to 1.0. The orthogonal loss weight  $\alpha_o$  is configured as 2.0 and 1.0 for latent-aware and semantic-aware training, respectively. For compositional and multi-concept motion generation, we directly use the model pre-trained on HumanML3D [18] and evaluate it on MTT [46] and our

DeCompML. Ablation studies on these hyperparameters, along with additional implementation details, are provided in the appendix.

## 4.3. Text-to-Motion Generation

**Quantitative results.** We compare our approach with recent state-of-the-art (SOTA) methods, *e.g.*, SALAD [24] and EnergyMoGen [71], on the HumanML3D [18] test set. The results are summarized in Table 1, from which we find that: *i*) By promoting the decompositional modeling, our compositional training paradigm effectively improves text-to-motion generation. This is particularly shown by DEMOGEN-OSS’s superior performance in terms of text-motion consistency, achieved while maintaining comparable FID scores against baselines. *ii*) The latent-aware DEMOGEN holds an advantage in generating smoother motion compared to the semantic-aware models, as reflected by its lower FID score. Note that our approach can be seamlessly integrated with other diffusion methods, *e.g.*, MLD [66] and MotionDiffuse [72], and results are provided in Appendix H.

**Motion Generation with Decompositional Understanding.** In Figure 3, we show how our approach infers a set of motion concepts from the given textual descriptions. These concepts can subsequently be composed to generate the target motion sequence. DEMOGEN-EXP requires the decompositional text from DeCompML as explicit input, while DEMOGEN-OSS and DEMOGEN-SC enable the motion generation without such decompositional guidance. As expected, all three variants effectively discover the compositional motion concepts intrinsic to the text-motion correspondence. These qualitative observations reinforce the quantitative results, further showing that our training paradigm endows the models with the capability of decompositional understanding.

Methods	Top-1 $\uparrow$	FID $\downarrow$	MM-Dist $\downarrow$
EnergyMoGen	0.326 $\pm$ .009	2.502 $\pm$ .028	4.348 $\pm$ .008
SALAD	0.342 $\pm$ .007	1.267 $\pm$ .024	4.282 $\pm$ .018
Ours (latent)	0.559 $\pm$ .004	<b>0.089</b> $\pm$ .005	2.758 $\pm$ .014
Ours (semantic)	<b>0.567</b> $\pm$ .004	0.102 $\pm$ .007	<b>2.719</b> $\pm$ .009

Table 3. **Motion composition on DeCompML.** We use the pre-trained text-to-motion model on HumanML3D for quantitative evaluation. As a baseline, SALAD [24] is modified to incorporate the compositional strategy from EnergyMoGen [71].

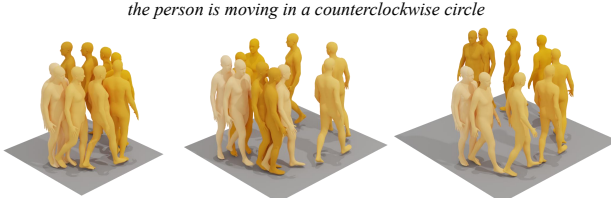


Figure 5. **Motion Diversity.** From left to right, we visualize the motions generated by DEMOGEN-OSS under a latent-aware setting for inferred concept 1, concept 2, and their combination.

#### 4.4. Motion Decomposition and Composition

**Decomposition and Recombination.** In Figure 4(a), we illustrate how our approach (latent-aware DEMOGEN-EXP), decomposes a complex motion into diverse and semantically interpretable sets of motion concepts guided by different decompositional texts. These results highlight the flexibility of our model in performing motion decomposition. Moreover, by recombining the decomposed concepts with others, our method is able to synthesize novel motions (as shown in Figure 4(b)) that do not appear in the training data. Collectively, these findings validate the effectiveness of our compositional training paradigm. More visual results of DEMOGEN-OSS and DEMOGEN-SC can be found on the [project page](#).

**Composition and Multi-concept generation.** Table 2 presents the results of our approach against SOTA diffusion models on MTT. Since DEMOGEN-EXP is trained directly with multiple textual descriptions, we use it to evaluate compositional motion generation. In contrast, the other two variants are more suitable for multi-concept generation. Our approach significantly outperforms prior SOTA models on both tasks. The results in Table 2 correspond to the latent-aware setting of DEMOGEN, which achieves better performance than EnergyMoGen across key evaluation metrics, such as R-Precision, TMR-Score, and FID.

Furthermore, our DeCompML dataset enables benchmarking for motion composition. Specifically, we construct compositional motion pairs by combining the textual annotations from DeCompML with motion samples from the HumanML3D [18] test set. We then compare the generated results against the corresponding HumanML3D ground-truth motion using the same evaluation model in

Methods	Top-1 $\uparrow$	FID $\downarrow$	MM-Dist $\downarrow$
EnergyMoGen	0.523 $\pm$ .003	0.188 $\pm$ .006	2.915 $\pm$ .007
EnergyMoGen*	0.526 $\pm$ .004	0.147 $\pm$ .004	2.884 $\pm$ .009
SALAD	0.581 $\pm$ .003	0.076 $\pm$ .002	2.649 $\pm$ .009
SALAD*	0.580 $\pm$ .004	0.060 $\pm$ .005	2.651 $\pm$ .014

Table 4. **Text-to-motion evaluation on extended HumanML3D.** \* indicates the finetuned model. Additional metrics and results of other methods are provided in Appendix G.

text-to-motion. As shown in Table 3, our DEMOGEN-EXP exhibits substantial performance advantages over prior approaches. Additional experimental results and ablation studies are provided in the appendix.

#### 4.5. Discussion

**Motion Diversity.** We observe that many motions in HumanML3D are simple and not amenable to further decomposition. For such motions, both DEMOGEN-OSS and DEMOGEN-SC can generate different variations in their expression. As illustrated in Figure 5, the synthesized motions exhibit diversity in terms of circle size and displacement. These results validate the effectiveness of two loss terms, *i.e.*,  $\mathcal{L}_{SC}$  and  $\mathcal{L}_{Ortho}$ . Ablation studies on them are provided in Appendix C and D.

**Experiments on DeCompML.** We finetune the pretrained text-to-motion models by incorporating data from both HumanML3D and DeCompML. Table 4 shows that finetuning SALAD significantly reduces FID by around 21%, while Top1 and MM-Dist remain largely unchanged. Integrating DeCompML improves all metrics for EnergyMoGen. The findings indicate that our compositional training paradigm facilitates the generation of high-quality decomposed motions, which can be effectively used to augment the dataset.

### 5. Conclusion

In this paper, we propose a compositional training paradigm, DEMOGEN, and explore three regimes of compositional supervision for decompositional motion generation. Our approach is able to effectively decompose human motion into distinct motion concepts, which can be flexibly recombined with external concepts to synthesize novel motions. We introduce the DeCompML dataset to facilitate compositional training, which can also serve as a benchmark for motion composition. Experimental results demonstrate the superior performance of our approach across various tasks, particularly in compositional and multi-concept motion generation. Moreover, our investigation reveals that leveraging the decomposed motions as additional training data still yields benefits for text-to-motion performance.

## References

[1] Chaitanya Ahuja and Louis-Philippe Morency. Language2pose: Natural language grounded pose forecasting. In *International Conference on 3D Vision (3DV)*, 2019. 2

[2] Nikos Athanasiou, Mathis Petrovich, Michael J. Black, and G  l Varol. TEACH: Temporal Action Compositions for 3D Humans. In *International Conference on 3D Vision (3DV)*, 2022. 1, 3

[3] Nikos Athanasiou, Mathis Petrovich, Michael J. Black, and G  l Varol. SINC: Spatial composition of 3D human motions for simultaneous action generation. In *Proceedings of the International Conference on Computer Vision (ICCV)*, 2023. 1, 3

[4] Tom Brown, Benjamin Mann, Nick Ryder, Melanie Subbiah, Jared D Kaplan, Prafulla Dhariwal, Arvind Neelakantan, Pranav Shyam, Girish Sastry, Amanda Askell, et al. Language models are few-shot learners. In *Advances in Neural Information Processing Systems (NeurIPS)*, 2020. 2

[5] Huiwen Chang, Han Zhang, Lu Jiang, Ce Liu, and William T. Freeman. Maskgit: Masked generative image transformer. In *Proceedings of the Conference on Computer Vision and Pattern Recognition (CVPR)*, 2022. 2

[6] Yuren Cong, Martin Renqiang Min, Li Erran Li, Bodo Rosenhahn, and Michael Ying Yang. Attribute-centric compositional text-to-image generation. *arXiv preprint arXiv:2301.01413*, 2023. 3

[7] Rishabh Dabral, Muhammad Hamza Mughal, Vladislav Golyanik, and Christian Theobalt. Mofusion: A framework for denoising-diffusion-based motion synthesis. In *Proceedings of the Conference on Computer Vision and Pattern Recognition (CVPR)*, 2023. 3

[8] Yilun Du and Leslie Kaelbling. Compositional generative modeling: A single model is not all you need. *arXiv preprint arXiv:2402.01103*, 2024. 3

[9] Yilun Du and Igor Mordatch. Implicit generation and modeling with energy based models. *Advances in Neural Information Processing Systems (NeurIPS)*, 2019. 1, 3

[10] Yilun Du, Shuang Li, and Igor Mordatch. Compositional visual generation with energy based models. In *Advances in Neural Information Processing Systems (NeurIPS)*, 2020. 3

[11] Yilun Du, Shuang Li, Yash Sharma, Josh Tenenbaum, and Igor Mordatch. Unsupervised learning of compositional energy concepts. *Advances in Neural Information Processing Systems (NeurIPS)*, 2021. 3

[12] Weixi Feng, Xuehai He, Tsu-Jui Fu, Varun Jampani, Arjun Reddy Akula, Pradyumna Narayana, Sugato Basu, Xin Eric Wang, and William Yang Wang. Training-free structured diffusion guidance for compositional text-to-image synthesis. In *International Conference on Learning Representations (ICLR)*, 2023. 3

[13] Xuehao Gao, Yang Yang, Zhenyu Xie, Shaoyi Du, Zhongqian Sun, and Yang Wu. Guess: Gradually enriching synthesis for text-driven human motion generation. *IEEE Transactions on Visualization and Computer Graphics*, 2024. 3

[14] Timur Garipov, Sebastiaan De Peuter, Ge Yang, Vikas Garg, Samuel Kaski, and Tommi Jaakkola. Compositional sculpting of iterative generative processes. *Advances in Neural Information Processing Systems (NeurIPS)*, 2023. 3

[15] Anindita Ghosh, Noshaba Cheema, Cennet Oguz, Christian Theobalt, and Philipp Slusallek. Synthesis of compositional animations from textual descriptions. In *Proceedings of the International Conference on Computer Vision (ICCV)*, 2021. 2

[16] Purvi Goel, Kuan-Chieh Wang, C Karen Liu, and Kayvon Fatahalian. Iterative motion editing with natural language. In *ACM SIGGRAPH 2024 Conference Papers*, 2024. 3

[17] Albert Gu and Tri Dao. Mamba: Linear-time sequence modeling with selective state spaces. *arXiv preprint arXiv:2312.00752*, 2023. 3

[18] Chuan Guo, Shihao Zou, Xinxin Zuo, Sen Wang, Wei Ji, Xingyu Li, and Li Cheng. Generating diverse and natural 3d human motions from text. In *Proceedings of the Conference on Computer Vision and Pattern Recognition (CVPR)*, 2022. 2, 5, 6, 7, 8, 15, 16

[19] Chuan Guo, Xinxin Zuo, Sen Wang, and Li Cheng. Tm2t: Stochastic and tokenized modeling for the reciprocal generation of 3d human motions and texts. In *Proceedings of the European Conference on Computer Vision (ECCV)*, 2022. 2

[20] Chuan Guo, Yuxuan Mu, Muhammad Gohar Javed, Sen Wang, and Li Cheng. Momask: Generative masked modeling of 3d human motions. In *Proceedings of the Conference on Computer Vision and Pattern Recognition (CVPR)*, 2024. 1, 2, 3

[21] Bo Han, Hao Peng, Minjing Dong, Yi Ren, Yixuan Shen, and Chang Xu. Amd: Autoregressive motion diffusion. In *Proceedings of the AAAI Conference on Artificial Intelligence*, 2024. 3

[22] Erik H  rk  nen, Aaron Hertzmann, Jaakko Lehtinen, and Sylvain Paris. Ganspace: Discovering interpretable gan controls. *Advances in Neural Information Processing Systems (NeurIPS)*, 2020. 3

[23] Jonathan Ho, Ajay Jain, and Pieter Abbeel. Denoising diffusion probabilistic models. In *Advances in Neural Information Processing Systems (NeurIPS)*, 2020. 1, 3

[24] Seokhyeon Hong, Chaelin Kim, Serin Yoon, Junghyun Nam, Sihun Cha, and Junyong Noh. Salad: Skeleton-aware latent diffusion for text-driven motion generation and editing. In *Proceedings of the Conference on Computer Vision and Pattern Recognition (CVPR)*, 2025. 3, 4, 5, 7, 8, 12, 17

[25] Benjamin Hoover, Yuchen Liang, Bao Pham, Rameswar Panda, Hendrik Strobelt, Duen Horng Chau, Mohammed Zaki, and Dmitry Krotov. Energy transformer. *Advances in Neural Information Processing Systems (NeurIPS)*, 2024. 3

[26] Jerry Yao-Chieh Hu, Dennis Wu, and Han Liu. Provably optimal memory capacity for modern hopfield models: Transformer-compatible dense associative memories as spherical codes. *arXiv preprint arXiv:2410.23126*, 2024. 3

[27] Jerry Yao-Chieh Hu, Weimin Wu, Zhuoru Li, Sophia Pi, Zhao Song, and Han Liu. On statistical rates and provably efficient criteria of latent diffusion transformers (dits). *Advances in Neural Information Processing Systems (NeurIPS)*, 2024. 3

[28] Biao Jiang, Xin Chen, Wen Liu, Jingyi Yu, Gang Yu, and Tao Chen. Motiongpt: Human motion as a foreign language. *arXiv*, 2023. 2

[29] Peng Jin, Yang Wu, Yanbo Fan, Zhongqian Sun, Wei Yang, and Li Yuan. Act as you wish: Fine-grained control of motion diffusion model with hierarchical semantic graphs. *Advances in Neural Information Processing Systems (NeurIPS)*, 2023. 3

[30] Korrawe Karunratanakul, Konpat Preechakul, Supasorn Suwajanakorn, and Siyu Tang. Guided motion diffusion for controllable human motion synthesis. In *Proceedings of the International Conference on Computer Vision (ICCV)*, 2023. 3

[31] Korrawe Karunratanakul, Konpat Preechakul, Supasorn Suwajanakorn, and Siyu Tang. Guided motion diffusion for controllable human motion synthesis. In *Proceedings of the International Conference on Computer Vision (ICCV)*, 2023. 1

[32] Hanyang Kong, Kehong Gong, Dongze Lian, Michael Bi Mi, and Xinchao Wang. Priority-centric human motion generation in discrete latent space. In *Proceedings of the Conference on Computer Vision and Pattern Recognition (CVPR)*, 2023. 3

[33] Yann LeCun, Sumit Chopra, Raia Hadsell, M Ranzato, Fujie Huang, et al. A tutorial on energy-based learning. *Predicting structured data*, 2006. 1

[34] Zhiheng Li, Martin Renqiang Min, Kai Li, and Chenliang Xu. Stylet2i: Toward compositional and high-fidelity text-to-image synthesis. In *Proceedings of the Conference on Computer Vision and Pattern Recognition (CVPR)*, 2022. 3

[35] Nan Liu, Shuang Li, Yilun Du, Josh Tenenbaum, and Antonio Torralba. Learning to compose visual relations. *Advances in Neural Information Processing Systems (NeurIPS)*, 2021. 3

[36] Nan Liu, Shuang Li, Yilun Du, Antonio Torralba, and Joshua B Tenenbaum. Compositional visual generation with composable diffusion models. In *Proceedings of the European Conference on Computer Vision (ECCV)*, 2022. 3

[37] Nan Liu, Yilun Du, Shuang Li, Joshua B Tenenbaum, and Antonio Torralba. Unsupervised compositional concepts discovery with text-to-image generative models. In *Proceedings of the International Conference on Computer Vision (ICCV)*, 2023. 3

[38] Yunhong Lou, Linchao Zhu, Yaxiong Wang, Xiaohan Wang, and Yi Yang. Diversemotion: Towards diverse human motion generation via discrete diffusion. *arXiv preprint arXiv:2309.01372*, 2023. 3

[39] Shunlin Lu, Ling-Hao Chen, Ailing Zeng, Jing Lin, Ruimao Zhang, Lei Zhang, and Heung-Yeung Shum. Humanantomato: Text-aligned whole-body motion generation. *arxiv:2310.12978*, 2023. 2

[40] OpenAI. Gpt-4 technical report. *arXiv preprint arXiv:2303.08774*, 2024. 6

[41] Geon Yeong Park, Jeongsol Kim, Beomsu Kim, Sang Wan Lee, and Jong Chul Ye. Energy-based cross attention for bayesian context update in text-to-image diffusion models. *Advances in Neural Information Processing Systems (NeurIPS)*, 2024. 3

[42] William Peebles, John Peebles, Jun-Yan Zhu, Alexei Efros, and Antonio Torralba. The hessian penalty: A weak prior for unsupervised disentanglement. In *Proceedings of the European Conference on Computer Vision (ECCV)*, 2020. 3

[43] Mathis Petrovich, Michael J. Black, and G  l Varol. Action-conditioned 3D human motion synthesis with transformer VAE. In *Proceedings of the International Conference on Computer Vision (ICCV)*, 2021. 2

[44] Mathis Petrovich, Michael J. Black, and Gul Varol. TEMOS: Generating diverse human motions from textual descriptions. In *Proceedings of the European Conference on Computer Vision (ECCV)*, 2022. 1

[45] Mathis Petrovich, Michael J Black, and G  l Varol. Tmr: Text-to-motion retrieval using contrastive 3d human motion synthesis. In *Proceedings of the International Conference on Computer Vision (ICCV)*, 2023. 2, 17

[46] Mathis Petrovich, Or Litany, Umar Iqbal, Michael J. Black, G  l Varol, Xue Bin Peng, and Davis Rempe. Multi-track timeline control for text-driven 3d human motion generation. In *Proceedings of the Conference on Computer Vision and Pattern Recognition Workshops (CVPRW)*, 2024. 1, 2, 6, 7, 15, 16, 17

[47] Ekkasit Pinyoanuntapong, Muhammad Usama Saleem, Korrawe Karunratanakul, Pu Wang, Hongfei Xue, Chen Chen, Chuan Guo, Junli Cao, Jian Ren, and Sergey Tulyakov. Controlmm: Controllable masked motion generation. *arXiv preprint arXiv:2410.10780*, 2024. 3

[48] Ekkasit Pinyoanuntapong, Pu Wang, Minwoo Lee, and Chen Chen. Mmm: Generative masked motion model. In *Proceedings of the Conference on Computer Vision and Pattern Recognition (CVPR)*, 2024. 2

[49] Konpat Preechakul, Nattanat Chathee, Suttisak Wizadwongsu, and Supasorn Suwajanakorn. Diffusion autoencoders: Toward a meaningful and decodable representation. In *Proceedings of the Conference on Computer Vision and Pattern Recognition (CVPR)*, 2022. 3

[50] Hubert Ramsauer, Bernhard Sch  fl, Johannes Lehner, Philipp Seidl, Michael Widrich, Thomas Adler, Lukas Gruber, Markus Holzleitner, Milena Pavlovi , Geir Kjetil Sandve, et al. Hopfield networks is all you need. *arXiv preprint arXiv:2008.02217*, 2020. 3

[51] Zeping Ren, Shaoli Huang, and Xiu Li. Realistic human motion generation with cross-diffusion models. *arXiv preprint arXiv:2312.10993*, 2023. 3

[52] Robin Rombach, Andreas Blattmann, Dominik Lorenz, Patrick Esser, and Bj  rn Ommer. High-resolution image synthesis with latent diffusion models. In *Proceedings of the Conference on Computer Vision and Pattern Recognition (CVPR)*, 2022. 1, 3

[53] Yoni Shafir, Guy Tevet, Roy Kapon, and Amit Haim Bermano. Human motion diffusion as a generative prior. In *International Conference on Learning Representations (ICLR)*, 2024. 1, 3

[54] Yujun Shen, Jinjin Gu, Xiaou Tang, and Bolei Zhou. Interpreting the latent space of gans for semantic face editing. In *Proceedings of the Conference on Computer Vision and Pattern Recognition (CVPR)*, 2020. 3

[55] Changhao Shi, Haomiao Ni, Kai Li, Shaobo Han, Mingfu Liang, and Martin Renqiang Min. Exploring compositional visual generation with latent classifier guidance. In *Proceedings of the Conference on Computer Vision and Pattern Recognition (CVPR)*, 2023. 3

[56] Krishna Kumar Singh, Utkarsh Ojha, and Yong Jae Lee. Finegan: Unsupervised hierarchical disentanglement for fine-grained object generation and discovery. In *Proceedings of the Conference on Computer Vision and Pattern Recognition (CVPR)*, 2019. 3

[57] Jascha Sohl-Dickstein, Eric Weiss, Niru Maheswaranathan, and Surya Ganguli. Deep unsupervised learning using nonequilibrium thermodynamics. In *International Conference on Machine Learning (ICML)*, 2015. 1

[58] Yang Song, Jascha Sohl-Dickstein, Diederik P Kingma, Abhishek Kumar, Stefano Ermon, and Ben Poole. Score-based generative modeling through stochastic differential equations. *arXiv preprint arXiv:2011.13456*, 2020. 3

[59] Jocelin Su, Nan Liu, Yanbo Wang, Joshua B Tenenbaum, and Yilun Du. Compositional image decomposition with diffusion models. *arXiv preprint arXiv:2406.19298*, 2024. 3, 5, 7

[60] Guy Tevet, Brian Gordon, Amir Hertz, Amit H Bermano, and Daniel Cohen-Or. Motionclip: Exposing human motion generation to clip space. In *Proceedings of the European Conference on Computer Vision (ECCV)*, 2022. 2

[61] Guy Tevet, Sigal Raab, Brian Gordon, Yonatan Shafir, Amit H Bermano, and Daniel Cohen-Or. Human motion diffusion model. *arXiv*, 2022. 1, 3, 5, 7

[62] Yin Wang, Zhiying Leng, Frederick WB Li, Shun-Cheng Wu, and Xiaohui Liang. Fg-t2m: Fine-grained text-driven human motion generation via diffusion model. In *Proceedings of the International Conference on Computer Vision (ICCV)*, 2023. 3

[63] Max Welling and Yee W Teh. Bayesian learning via stochastic gradient langevin dynamics. In *International Conference on Machine Learning (ICML)*, 2011. 3

[64] Yiming Xie, Varun Jampani, Lei Zhong, Deqing Sun, and Huaizu Jiang. Omnicontrol: Control any joint at any time for human motion generation. *arXiv preprint arXiv:2310.08580*, 2023. 1, 3

[65] Zhenyu Xie, Yang Wu, Xuehao Gao, Zhongqian Sun, Wei Yang, and Xiaodan Liang. Towards detailed text-to-motion synthesis via basic-to-advanced hierarchical diffusion model. In *Proceedings of the AAAI Conference on Artificial Intelligence*, 2024. 3

[66] Chen Xin, Biao Jiang, Wen Liu, Zilong Huang, Bin Fu, Tao Chen, Jingyi Yu, and Gang Yu. Executing your commands via motion diffusion in latent space. *arXiv*, 2022. 1, 3, 5, 7, 12, 14, 18

[67] Zhao Yang, Bing Su, and Ji-Rong Wen. Synthesizing long-term human motions with diffusion models via coherent sampling. In *Proceedings of the ACM International Conference on Multimedia (ACMMM)*, 2023. 3

[68] Ye Yuan, Jiaming Song, Umar Iqbal, Arash Vahdat, and Jan Kautz. Physdiff: Physics-guided human motion diffusion model. In *Proceedings of the International Conference on Computer Vision (ICCV)*, 2023.

[69] Yuanhao Zhai, Mingzhen Huang, Tianyu Luan, Lu Dong, Ifeoma Nwogu, Siwei Lyu, David Doermann, and Junsong Yuan. Language-guided human motion synthesis with atomic actions. In *Proceedings of the ACM International Conference on Multimedia (ACMMM)*, 2023. 3

[70] Jianrong Zhang, Yangsong Zhang, Xiaodong Cun, Yong Zhang, Hongwei Zhao, Hongtao Lu, Xi Shen, and Ying Shan. Generating human motion from textual descriptions with discrete representations. In *Proceedings of the Conference on Computer Vision and Pattern Recognition (CVPR)*, 2023. 1, 2, 3, 14, 17

[71] Jianrong Zhang, Hehe Fan, and Yi Yang. Energymogen: Compositional human motion generation with energy-based diffusion model in latent space. In *Proceedings of the Conference on Computer Vision and Pattern Recognition (CVPR)*, 2025. 1, 2, 3, 4, 5, 7, 8, 12, 17

[72] Mingyuan Zhang, Zhongang Cai, Liang Pan, Fangzhou Hong, Xinying Guo, Lei Yang, and Ziwei Liu. Motiondiffuse: Text-driven human motion generation with diffusion model. *arXiv*, 2022. 1, 3, 7, 12, 14, 18

[73] Mingyuan Zhang, Xinying Guo, Liang Pan, Zhongang Cai, Fangzhou Hong, Huirong Li, Lei Yang, and Ziwei Liu. Remodiffuse: Retrieval-augmented motion diffusion model. *arXiv*, 2023. 1, 3, 5, 7

[74] Mingyuan Zhang, Huirong Li, Zhongang Cai, Jiawei Ren, Lei Yang, and Ziwei Liu. Finemogen: Fine-grained spatio-temporal motion generation and editing. *Advances in Neural Information Processing Systems (NeurIPS)*, 2023. 3, 5, 7

[75] Yaqi Zhang, Di Huang, Bin Liu, Shixiang Tang, Yan Lu, Lu Chen, Lei Bai, Qi Chu, Nenghai Yu, and Wanli Ouyang. Motiongpt: Finetuned llms are general-purpose motion generators. *arXiv*, 2023. 2

[76] Zeyu Zhang, Akide Liu, Ian Reid, Richard Hartley, Bohan Zhuang, and Hao Tang. Motion mamba: Efficient and long sequence motion generation. In *European Conference on Computer Vision*, pages 265–282. Springer, 2025. 3

[77] Junbo Zhao, Michael Mathieu, and Yann LeCun. Energy-based generative adversarial networks. In *International Conference on Learning Representations (ICLR)*, 2017. 1

[78] Chongyang Zhong, Lei Hu, Zihao Zhang, and Shihong Xia. Attt2m: Text-driven human motion generation with multi-perspective attention mechanism. In *Proceedings of the International Conference on Computer Vision (ICCV)*, 2023. 1, 2

[79] Zixiang Zhou and Baoyuan Wang. Ude: A unified driving engine for human motion generation. In *Proceedings of the Conference on Computer Vision and Pattern Recognition (CVPR)*, 2023. 3

## Appendix

In this appendix, we present:

- Section **A**: Training and inference details of DEMOGEN.
- Section **B**: Ablations on the hyper-parameters of DEMOGEN-EXP
- Section **C**: Ablations on orthogonalization loss  $\mathcal{L}_{\text{Ortho}}$  weight  $\alpha_o$  for DEMOGEN-OSS.
- Section **D**: Ablations on orthogonalization loss  $\mathcal{L}_{\text{Ortho}}$  weight  $\alpha_o$  and semantic consistency loss  $\mathcal{L}_{\text{SC}}$  weight  $\alpha_{\text{sc}}$  for DEMOGEN-SC.
- Section **E**: Additional results of multi-concept motion generation.
- Section **F**: Ablation studies on the number of decomposed motion concepts  $K$ .
- Section **G**: Text-to-motion evaluation on the extended HumanML3D, *i.e.*, DeCompML.
- Section **H**: Additional results of our compositional training paradigm on MLD and MotionDiffuse
- Section **I**: More details on datasets and evaluation metrics.

## A. Implementation Details

### A.1. Training

For motion VAE, we apply downsampling in both the temporal and spatial dimensions to obtain a latent feature  $\mathbf{z} \in \mathbb{R}^{L' \times N_j \times d'_m}$ , where  $L'$  is the latent feature length with a downsampling rate of 4.  $N_j$  and  $d'_m$  denote the number of joints and latent feature dimension, which are set to 7 and 32, respectively. The VAE is initialized with pretrained weights from [24] for fair comparison. For the diffusion model, we use a 5-layer transformer with a dimension of 256. The learning rate is initialized at 0.0002 and subsequently reduced to 0.00002 following 50,000 training iterations.

On the extended HumanML3D dataset, *i.e.*, DeCompML, we finetune the latent diffusion models of two recent state-of-the-art approaches, EnergyMoGen [71] and SALAD [24], for 100K iterations and 300 epochs. The learning rates are set to 0.00001 and 0.00002, respectively. For the experiments in Section **H**, we apply our compositional training paradigm to two classic and representative

methods: MLD [66] and MotionDiffuse [72]. We follow their original training configurations.

### A.2. Inference

During inference, we sample 50 diffusion steps to generate motion from texts. The pseudocode for text-to-motion generation (DEMOGEN-EXP, -OSS, -SC) and compositional motion generation (DEMOGEN-EXP) inference is illustrated in Algorithm 2. Note that DEMOGEN-EXP adopts a text replacement rate  $\tau$  during training, enabling high-quality text-to-motion generation by duplicating the single textual description. The ablation study for  $\tau$  is provided in Section **B**. Furthermore, Algorithm 3 presents the pseudocode for decompositional motion generation, where decomposed concepts can be recombined using Algorithm 2.

## B. Ablations on DEMOGEN-EXP

We conduct ablative experiments for DEMOGEN-EXP on HumanML3D, DeCompML, and MTT. Text-to-motion results are provided in Table 5. As  $\tau$  increases from 0.0 to 0.7, we observe that the model consistently shows improved R-Precision, FID, and MM-Dist. The results for compositional motion generation on the DeCompML dataset (in Table 6) demonstrate similar findings.  $\tau = 0.7$  achieves the best results under both latent-aware and semantic-aware settings. We also investigate the impact of  $\tau$  on a more complicated benchmark, *i.e.*, MTT. As shown in Table 7, we find that the latent-aware DEMOGEN-EXP significantly outperforms the current state-of-the-art model, *i.e.*, EnergyMoGen [71] across all settings of  $\tau$ . As for the semantic-aware model, we achieve improvements in most metrics, such as R-Precision, TMR-Score, and Transition distance, except for a decline in FID.

It is worth noting that the semantic-aware model performs better when the input conditions remain within the training distribution (HumanML3D and DeCompML). In contrast, the latent-aware model demonstrates stronger generalization in out-of-domain scenarios (MTT). Please note that all experimental results in Table 5–7 are obtained using models trained on the HumanML3D dataset (with decomposed textual descriptions from DeCompML).

## C. Ablations on DEMOGEN-OSS

We study the impact of orthogonalization loss weight  $\alpha_o$  in DEMOGEN-OSS, and the results are reported in Table 8. All tested values of  $\alpha_o$  deliver competitive performance. Notably,  $\alpha_o = 2.0$  yields the best performance for the latent-aware configuration, while  $\alpha_o = 1.0$  performs best under the semantic-aware setting.

---

**Algorithm 2** Text-to-Motion Generation and Compositional Motion Generation

---

```
1: Require: Frozen VAE decoder  $\mathcal{D}$ , denoising network  $\epsilon_\theta$ , diffusion timestep  $T$ , text
   embeddings  $C = \{c_k\}_{k=1}^K$ , a latent feature  $\mathbf{z}_T \sim \mathcal{N}(0, 1)$ 
2: for  $t = T, \dots, 1$  do
3:   if mod is latent-aware then
4:      $\epsilon_{pred} \leftarrow \sum_{k=1}^K \epsilon_\theta(\mathbf{z}_t, c_k, t)$ 
5:   end if
6:   if mod is semantic-aware then
7:      $\epsilon_{pred} \leftarrow \epsilon_\theta(\mathbf{z}_t, C, t)$  // Replace the cross-attention with DCA
8:   end if
9:   // Run denoising step
10:   $\mathbf{z}_{t-1} = \frac{1}{\sqrt{\alpha_t}}(\mathbf{z}_t - \eta_t \epsilon_{pred}) + \mathcal{N}(0, \hat{\beta}_t I)$ .
11:  where  $\alpha_t = 1 - \beta_t$ ,  $\bar{\alpha}_t = \prod_{i=1}^t \alpha_i$ , and  $\eta_t = \frac{1 - \alpha_t}{\sqrt{1 - \bar{\alpha}_t}}$ .
12: end for
```

---

---

**Algorithm 3** Decompositional Motion Generation

---

```
Require: Frozen VAE decoder  $\mathcal{D}$ , denoising network  $\epsilon_\theta$ , diffusion timestep  $T$ , text
   embeddings  $C = \{c_k\}_{k=1}^K$ , a set of latent features  $\{\mathbf{z}_T^k\}_{k=1}^K$  with  $\mathbf{z}_T^k \sim \mathcal{N}(0, 1)$ 
2: for  $t = T, \dots, 1$  do
   // For both latent-aware and semantic-aware settings
4:   for  $k = 1, \dots, K$  do
5:      $\epsilon_{pred}^k \leftarrow \epsilon_\theta(\mathbf{z}_t^k, c_k, t)$ 
6:     // Run denoising step
7:      $\mathbf{z}_{t-1}^k = \frac{1}{\sqrt{\alpha_t}}(\mathbf{z}_t^k - \eta_t \epsilon_{pred}^k) + \mathcal{N}(0, \hat{\beta}_t I)$ .
8:     where  $\alpha_t = 1 - \beta_t$ ,  $\bar{\alpha}_t = \prod_{i=1}^t \alpha_i$ , and  $\eta_t = \frac{1 - \alpha_t}{\sqrt{1 - \bar{\alpha}_t}}$ .
   end for
10: end for
```

---

## D. Ablations on Loss Weights $\alpha_{sc}$ and $\alpha_o$ for DEMOGEN-SC

The results are provided in Table 9. We first conduct an ablation study on the scaling loss weight  $\alpha_{sc}$ , building on the findings presented in Section C. We then further examine the performance of the model without orthogonalization loss. For the latent-aware DEMOGEN-SC, although setting  $\alpha_{sc}$  to 1 slightly degrades performance, we retain this value to encourage the model to learn from the decomposed text. Conversely, for the semantic-aware model, setting  $\alpha_{sc}$  to 1 achieves the best performance. Meanwhile, the performance decreases when the orthogonalization loss is removed, further demonstrating its effectiveness.

## E. Additional Results of Multi-concept Motion Generation

The results are shown in Table 10. We observe that the semantic-aware setting surpasses the latent-aware setting on both DEMOGEN-OSS and DEMOGEN-SC, indicating its

stronger ability to generate motions from a single complex textual description. Please refer to Table 7 for the results and analysis of motion composition.

## F. Ablation Studies on the Number of Decomposed Motion Concepts $K$

We explore the effect of the number of decomposed motion concepts  $K$  on HumanML3D. GPT-4.1 is used to generate decomposed texts with three or four components (see Section I for more details), and a latent-aware DEMOGEN-EXP is trained accordingly. As shown in Table 11, with an increasing number of decomposed motion concepts  $K$ , several key metrics, including FID and R-Precision, consistently decline on DEMOGEN-EXP. We believe that the decrease is mainly due to the limited information in HumanML3D texts, which constrains the extraction of high-quality components under three- or four-part decompositions. To verify this, we further conduct experiments on DEMOGEN-OSS, which does not require decomposed textual instructions. We find that  $K = 4$  achieves performance

$\tau$	R-Precision $\uparrow$			FID $\downarrow$	MM-Dist $\downarrow$	Diversity $\rightarrow$
	Top-1	Top-2	Top-3			
<b><i>latent-aware</i></b>						
0.0	$0.532 \pm .005$	$0.726 \pm .004$	$0.820 \pm .003$	$0.255 \pm .012$	$2.926 \pm .012$	<b><math>9.707 \pm .111</math></b>
0.3	$0.562 \pm .004$	$0.756 \pm .004$	$0.844 \pm .003$	$0.108 \pm .004$	<u><math>2.753 \pm .017</math></u>	<u><math>9.766 \pm .104</math></u>
0.5	<u><math>0.565 \pm .004</math></u>	<u><math>0.757 \pm .003</math></u>	<u><math>0.845 \pm .003</math></u>	<u><math>0.095 \pm .004</math></u>	$2.757 \pm .011$	$9.849 \pm .102$
0.7	<b><math>0.569 \pm .004</math></b>	<b><math>0.760 \pm .005</math></b>	<b><math>0.850 \pm .004</math></b>	<b><math>0.078 \pm .003</math></b>	<b><math>2.708 \pm .012</math></b>	$9.774 \pm .099$
<b><i>semantic-aware</i></b>						
0.0	$0.564 \pm .003$	$0.756 \pm .004$	$0.845 \pm .002$	$0.297 \pm .016$	$2.764 \pm .012$	<b><math>9.784 \pm .057</math></b>
0.3	$0.579 \pm .004$	$0.769 \pm .003$	$0.858 \pm .003$	$0.118 \pm .007$	$2.694 \pm .009$	$9.858 \pm .054$
0.5	<u><math>0.583 \pm .002</math></u>	<u><math>0.774 \pm .004</math></u>	<b><math>0.865 \pm .002</math></b>	<b><math>0.100 \pm .006</math></b>	<u><math>2.632 \pm .006</math></u>	<u><math>9.807 \pm .063</math></u>
0.7	<b><math>0.586 \pm .005</math></b>	<b><math>0.776 \pm .003</math></b>	$0.863 \pm .002$	$0.116 \pm .008$	<b><math>2.623 \pm .008</math></b>	$9.873 \pm .057$

Table 5. **Ablation of text replacement rate  $\tau$  in DEMOGEN-EXP for text-to-motion on the HumanML3D test set.** **Bold** and underlined denote the best and second-best results, respectively.

$\tau$	R-Precision $\uparrow$			FID $\downarrow$	MM-Dist $\downarrow$	Diversity $\rightarrow$
	Top-1	Top-2	Top-3			
<b><i>latent-aware</i></b>						
0.0	$0.544 \pm .005$	$0.738 \pm .005$	$0.830 \pm .003$	<b><math>0.089 \pm .006</math></b>	$2.850 \pm .010$	<b><math>9.703 \pm .090</math></b>
0.3	<u><math>0.551 \pm .005</math></u>	<u><math>0.743 \pm .006</math></u>	<u><math>0.834 \pm .004</math></u>	$0.109 \pm .007$	<u><math>2.817 \pm .023</math></u>	<u><math>9.735 \pm .104</math></u>
0.5	$0.550 \pm .004$	<u><math>0.743 \pm .002</math></u>	<u><math>0.834 \pm .003</math></u>	<u><math>0.093 \pm .007</math></u>	<u><math>2.817 \pm .015</math></u>	$9.803 \pm .105$
0.7	<b><math>0.559 \pm .004</math></b>	<b><math>0.754 \pm .004</math></b>	<b><math>0.842 \pm .004</math></b>	<b><math>0.089 \pm .005</math></b>	<b><math>2.758 \pm .014</math></b>	$9.756 \pm .115$
<b><i>semantic-aware</i></b>						
0.0	$0.547 \pm .004$	$0.737 \pm .002$	$0.827 \pm .004$	$0.163 \pm .010$	$2.826 \pm .007$	$9.864 \pm .056$
0.3	$0.561 \pm .005$	$0.750 \pm .003$	$0.841 \pm .003$	$0.111 \pm .006$	$2.765 \pm .010$	$9.809 \pm .062$
0.5	<u><math>0.565 \pm .004</math></u>	<u><math>0.757 \pm .004</math></u>	<u><math>0.845 \pm .003</math></u>	<b><math>0.095 \pm .006</math></b>	<u><math>2.720 \pm .012</math></u>	<b><math>9.771 \pm .056</math></b>
0.7	<b><math>0.567 \pm .004</math></b>	<b><math>0.760 \pm .003</math></b>	<b><math>0.846 \pm .002</math></b>	<u><math>0.102 \pm .007</math></u>	<b><math>2.719 \pm .009</math></b>	$9.786 \pm .058$

Table 6. **Ablation of text replacement rate  $\tau$  in DEMOGEN-EXP for motion composition on DeCompML.**

comparable to that of  $K = 2$ . Furthermore,  $K = 2$  also enables a larger number of concept compositions through iterative aggregation of energy scores.

## G. Text-to-motion Evaluation on the DeCompML Dataset

In Section 4.5, we demonstrate that leveraging the decomposed motions as additional training data can improve text-to-motion performance. In this section, we provide complementary evaluation metrics and further validate our dataset by presenting results on a classical VQ-VAE-based approach, *i.e.*, T2M-GPT [70] (as shown in Figure 12). The improvement for SALAD is mainly reflected in the FID metric, which we attribute to its already strong performance in terms of R-precision and MM-Dist. Both T2M-GPT and EnergyMoGen show improvements in motion smoothness

(FID) and text–motion consistency (R-precision and MM-Dist).

## H. Additional Results of Our Compositional Training Paradigm on MLD and Motion-Diffuse

To comprehensively validate our approach, we apply the compositional training paradigm to MLD [66] and Motion-Diffuse [72], the results are presented in Table 13. We train both models based on orthogonal self-supervision (OSS) under a latent-aware setting. Notably, we find that MotionDiffuse achieves better performance when predicting  $\mathbf{x}_0$ . The experimental results demonstrate that our approach serves as a general training paradigm, which can be seamlessly integrated with existing diffusion models.

Methods	R-Precision		TMR-Score ↑		FID ↓	Transition distance ↓
	R@1 ↑	R@3 ↑	M2T	M2M		
<i>latent-aware</i>						
EnergyMoGen (latent)	9.7	19.6	0.547	0.521	0.917	<u>1.6</u>
DEMOGEN-EXP ( $\tau=0.0$ )	<b>16.5</b>	<b>31.9</b>	0.594	0.566	0.630	1.7
DEMOGEN-EXP ( $\tau=0.3$ )	<u>16.3</u>	<u>31.7</u>	0.594	<b>0.570</b>	<b>0.607</b>	<u>1.6</u>
DEMOGEN-EXP ( $\tau=0.5$ )	15.3	31.1	<u>0.596</u>	0.563	0.648	<b>1.5</b>
DEMOGEN-EXP ( $\tau=0.7$ )	16.2	<b>31.9</b>	<b>0.597</b>	<b>0.570</b>	<u>0.621</u>	<u>1.6</u>
<i>semantic-aware</i>						
EnergyMoGen (semantic)	<u>15.1</u>	27.5	0.585	0.567	<b>0.569</b>	2.2
DEMOGEN-EXP ( $\tau=0.0$ )	13.5	27.1	0.577	0.560	<u>0.606</u>	<u>2.1</u>
DEMOGEN-EXP ( $\tau=0.3$ )	14.1	28.2	0.581	0.563	0.648	<b>1.8</b>
DEMOGEN-EXP ( $\tau=0.5$ )	<b>15.2</b>	<b>30.1</b>	<b>0.594</b>	0.564	0.643	<u>1.8</u>
DEMOGEN-EXP ( $\tau=0.7$ )	14.8	<u>29.3</u>	0.584	<b>0.568</b>	0.631	<b>1.8</b>

Table 7. **Quantitative comparison on the MTT [46] dataset.** We compare our approach with EnergyMoGen and analyze the impact of the text replacement rate  $\tau$ .

$\alpha_o$	R-Precision ↑			FID ↓	MM-Dist ↓	Diversity →
	Top-1	Top-2	Top-3			
<i>latent-aware</i>						
0.0	0.582 $\pm$ .005	0.771 $\pm$ .003	0.855 $\pm$ .003	0.138 $\pm$ .005	2.642 $\pm$ .008	9.851 $\pm$ .147
0.1	<u>0.584</u> $\pm$ .007	0.771 $\pm$ .005	0.857 $\pm$ .001	0.097 $\pm$ .004	2.641 $\pm$ .016	9.781 $\pm$ .096
0.5	<u>0.584</u> $\pm$ .003	<u>0.775</u> $\pm$ .004	<u>0.860</u> $\pm$ .003	<u>0.092</u> $\pm$ .005	<u>2.629</u> $\pm$ .009	<b>9.729</b> $\pm$ .145
1.0	0.583 $\pm$ .003	0.772 $\pm$ .005	0.857 $\pm$ .003	<b>0.074</b> $\pm$ .004	2.635 $\pm$ .009	9.799 $\pm$ .107
2.0	<b>0.588</b> $\pm$ .004	<b>0.778</b> $\pm$ .002	<b>0.861</b> $\pm$ .003	<u>0.092</u> $\pm$ .003	<b>2.625</b> $\pm$ .007	<u>9.779</u> $\pm$ .120
<i>semantic-aware</i>						
0.0	<u>0.583</u> $\pm$ .004	0.771 $\pm$ .003	0.856 $\pm$ .003	<b>0.093</b> $\pm$ .005	2.649 $\pm$ .009	<b>9.797</b> $\pm$ .123
0.1	<u>0.583</u> $\pm$ .005	<b>0.776</b> $\pm$ .002	<b>0.861</b> $\pm$ .003	0.113 $\pm$ .005	<u>2.648</u> $\pm$ .011	9.928 $\pm$ .112
0.5	<u>0.583</u> $\pm$ .003	<b>0.776</b> $\pm$ .003	<b>0.861</b> $\pm$ .002	0.112 $\pm$ .005	2.662 $\pm$ .010	9.929 $\pm$ .126
1.0	<b>0.584</b> $\pm$ .002	<u>0.774</u> $\pm$ .003	<u>0.858</u> $\pm$ .001	<u>0.104</u> $\pm$ .005	<b>2.637</b> $\pm$ .014	<u>9.877</u> $\pm$ .127
2.0	0.578 $\pm$ .004	0.769 $\pm$ .003	0.855 $\pm$ .004	0.107 $\pm$ .004	2.665 $\pm$ .010	9.905 $\pm$ .114

Table 8. **Ablation of orthogonalization loss weight  $\alpha_o$  for DEMOGEN-OSS on the HumanML3D test set.** We find that  $\alpha_o = 2$  and  $\alpha_o = 1$  yield the best performance for latent-aware and semantic-aware DEMOGEN-OSS, respectively.

## I. More Details on Datasets and Evaluation Metrics

### I.1. DeCompML

This section describes how decomposed text in DeCompML is generated. We utilize a large language model and design prompts to automatically perform the decomposition of the given text. The text prompt is shown in Table 14. We experiment with multiple large language models, including GPT-4o, GPT-4.1, GPT-5, and GPT-OSS-

120B (OpenAI’s 120B open-source model). GPT-OSS-120B and GPT-4o often fail to effectively decompose the text, frequently producing empty outputs. GPT-5 requires longer inference time and sometimes generates additional irrelevant content. Therefore, we ultimately select GPT-4.1 for our decomposition tasks.

### I.2. Evaluation Metrics

We evaluate text-driven human motion generation using the models and metrics from Guo *et al.* [18]. Motion quality

$\alpha_o$	$\alpha_{sc}$	R-Precision $\uparrow$			FID $\downarrow$	MM-Dist $\downarrow$	Diversity $\rightarrow$
		Top-1	Top-2	Top-3			
<b><i>latent-aware</i></b>							
2.0	0.1	<b>0.569</b> $\pm$ .002	<b>0.761</b> $\pm$ .004	<b>0.847</b> $\pm$ .006	<b>0.112</b> $\pm$ .006	<b>2.712</b> $\pm$ .016	<b>9.763</b> $\pm$ .125
2.0	0.5	0.560 $\pm$ .004	0.756 $\pm$ .003	0.846 $\pm$ .002	0.152 $\pm$ .004	2.754 $\pm$ .010	9.935 $\pm$ .116
2.0	1.0	0.565 $\pm$ .003	0.757 $\pm$ .004	0.846 $\pm$ .003	0.121 $\pm$ .005	2.739 $\pm$ .009	9.933 $\pm$ .131
0.0	1.0	0.560 $\pm$ .004	0.752 $\pm$ .004	0.845 $\pm$ .003	0.185 $\pm$ .008	2.742 $\pm$ .006	9.976 $\pm$ .151
<b><i>semantic-aware</i></b>							
1.0	0.1	0.564 $\pm$ .003	0.755 $\pm$ .006	0.845 $\pm$ .005	0.132 $\pm$ .007	2.741 $\pm$ .016	9.954 $\pm$ .182
1.0	0.5	0.557 $\pm$ .003	0.751 $\pm$ .002	0.841 $\pm$ .003	0.174 $\pm$ .006	2.774 $\pm$ .012	9.924 $\pm$ .154
1.0	1.0	<b>0.565</b> $\pm$ .002	<b>0.758</b> $\pm$ .003	<b>0.846</b> $\pm$ .003	0.138 $\pm$ .005	<b>2.727</b> $\pm$ .010	9.769 $\pm$ .158
0.0	1.0	0.561 $\pm$ .003	0.755 $\pm$ .004	0.844 $\pm$ .003	<b>0.080</b> $\pm$ .004	2.734 $\pm$ .009	<b>9.712</b> $\pm$ .145

Table 9. **Ablation of loss hyper-parameters in DEMOGEN-SC on the HumanML3D test set.**

Methods	R-Precision		TMR-Score $\uparrow$		FID $\downarrow$	Transition distance $\downarrow$
	R@1 $\uparrow$	R@3 $\uparrow$	M2T	M2M		
Multi-concept motion generation (single text)						
DEMOGEN-OSS(latent)	14.9	29.5	0.584	<b>0.57</b>	0.580	2.6
DEMOGEN-OSS (semantic)	<b>15.4</b>	29.2	<b>0.585</b>	0.571	0.598	<b>2.4</b>
DEMOGEN-SC (latent)	14.3	<b>29.7</b>	0.578	0.568	0.585	2.7
DEMOGEN-SC (semantic)	14.8	29.1	0.578	0.569	<b>0.575</b>	<b>2.6</b>

Table 10. **Quantitative results on MTT [46].** We present the multi-concept generation results of the semantic-aware DEMOGEN. The metrics are computed following STMC [46].

is measured by FID, text-motion alignment by R-Precision and MM-Dist, and diversity by Diversity and Multimodality metrics. The feature sets of ground-truth and generated motions are denoted as  $\mathbf{m}$  and  $\hat{\mathbf{m}}$ , respectively.

**R-Precision.** For each motion sequence, we use 32 text descriptions (one ground-truth and 31 randomly selected mismatched) and rank them based on the Euclidean distance between motion and text embeddings. We report Top-1, Top-2, and Top-3 accuracy for motion-to-text retrieval.

**FID.** The Fréchet Inception Distance (FID) serves as a key indicator of the realism and quality of synthetic motions. It calculates the statistical difference between the feature space of the generated samples ( $\hat{\mathbf{m}}$ ) and the real data ( $\mathbf{m}$ ):

$$\text{FID} = \|\mu_{\hat{\mathbf{m}}} - \mu_{\mathbf{m}}\|^2 + \text{TR}(\Sigma_{\hat{\mathbf{m}}} + \Sigma_{\mathbf{m}} - 2\sqrt{\Sigma_{\hat{\mathbf{m}}}\Sigma_{\mathbf{m}}}). \quad (6)$$

Here,  $\mu$  represents the feature set mean, and  $\Sigma$  is the covariance matrix. A key property is that lower values of FID imply higher fidelity to the real data distribution.

**MM-Dist.** We compute the average Euclidean distance between each text embedding and the corresponding motion embedding generated from that text, providing a measure of alignment between text and motion features.

**Diversity.** We quantify the variation of motions generated from different text descriptions in the test set by randomly sampling 300 motion pairs. For each pair, we compute the Euclidean distance between their feature representations, and define the Diversity metric as:

$$\text{Diversity} = \frac{1}{300} \sum_{i=1}^{300} \left\| \hat{\mathbf{m}}_1^{(i)} - \hat{\mathbf{m}}_2^{(i)} \right\|, \quad (7)$$

where  $\hat{\mathbf{m}}_1^{(i)}$  and  $\hat{\mathbf{m}}_2^{(i)}$  denote the motion features of the  $i$ -th pair.

**Multimodality.** To evaluate the variation among motions generated from the same textual description, we adopt a procedure similar to Diversity. Following Guo *et al.* [18], we generate multiple samples per text and partition them into two random subsets. The Multimodality metric is calculated as the average Euclidean distance between paired

K	R-Precision $\uparrow$			FID $\downarrow$	MM-Dist $\downarrow$	Diversity $\rightarrow$
	Top-1	Top-2	Top-3			
<b>DEMOGEN-EXP</b>						
2	<b>0.569<math>\pm</math>.004</b>	<b>0.760<math>\pm</math>.005</b>	<b>0.850<math>\pm</math>.004</b>	<b>0.078<math>\pm</math>.003</b>	<b>2.708<math>\pm</math>.012</b>	<b>9.774<math>\pm</math>.099</b>
3	<u>0.556<math>\pm</math>.005</u>	<u>0.749<math>\pm</math>.005</u>	<u>0.840<math>\pm</math>.003</u>	<u>0.110<math>\pm</math>.005</u>	<u>2.786<math>\pm</math>.016</u>	<u>9.822<math>\pm</math>.133</u>
4	0.553 $\pm$ .005	0.748 $\pm$ .004	0.836 $\pm$ .002	0.157 $\pm$ .005	2.795 $\pm$ .011	<b>9.743<math>\pm</math>.116</b>
<b>DEMOGEN-OSS</b>						
2	<b>0.588<math>\pm</math>.004</b>	<b>0.778<math>\pm</math>.002</b>	<u>0.861<math>\pm</math>.003</u>	<b>0.092<math>\pm</math>.003</b>	<b>2.625<math>\pm</math>.007</b>	<b>9.779<math>\pm</math>.120</b>
4	<u>0.584<math>\pm</math>.007</u>	<u>0.776<math>\pm</math>.002</u>	<b>0.862<math>\pm</math>.002</b>	<u>0.100<math>\pm</math>.006</u>	<u>2.636<math>\pm</math>.016</u>	<u>9.801<math>\pm</math>.247</u>

Table 11. **Ablation on the number of decomposed concepts  $K$  on the HumanML3D test set.**

Method	R-Precision $\uparrow$			FID $\downarrow$	MM-Dist $\downarrow$	Diversity $\rightarrow$
	Top-1	Top-2	Top-3			
T2M-GPT [70]	0.491 $\pm$ .003	0.680 $\pm$ .003	0.775 $\pm$ .002	0.116 $\pm$ .004	3.118 $\pm$ .011	9.761 $\pm$ .081
T2M-GPT [70]*	0.497 $\pm$ .004	0.685 $\pm$ .002	0.780 $\pm$ .003	0.102 $\pm$ .008	3.017 $\pm$ .007	9.748 $\pm$ .074
EnergyMoGen [71]	0.523 $\pm$ .003	0.715 $\pm$ .002	0.815 $\pm$ .002	0.188 $\pm$ .006	2.915 $\pm$ .007	9.488 $\pm$ .099
EnergyMoGen [71]*	0.526 $\pm$ .004	0.718 $\pm$ .002	0.818 $\pm$ .003	0.147 $\pm$ .004	2.884 $\pm$ .009	9.392 $\pm$ .084
SALAD [24]	0.581 $\pm$ .003	0.769 $\pm$ .003	0.857 $\pm$ .002	0.076 $\pm$ .002	2.649 $\pm$ .009	9.696 $\pm$ .096
SALAD [24]*	0.580 $\pm$ .003	0.769 $\pm$ .003	0.857 $\pm$ .003	0.060 $\pm$ .005	2.651 $\pm$ .009	9.379 $\pm$ .149

Table 12. **Quantitative comparison on the HumanML3D test set.** \* denotes that the model is finetuned on DeCompML.

features from these subsets, following the same formulation as the Diversity metric.

Following STMC [46] and EnergyMoGen [71], we evaluate compositional motion generation using R-Precision, TMR-Score, FID, and Transition Distance. The TMR-Score quantifies motion-text alignment via the cosine similarity of embeddings derived from the TMR model [45], similar to MM-Dist. Transition Distance is computed as the Euclidean distance between consecutive frames.

Method	R-Precision $\uparrow$			FID $\downarrow$	MM-Dist $\downarrow$	Diversity $\rightarrow$
	Top-1	Top-2	Top-3			
MLD [66]	0.481 $\pm$ .003	0.673 $\pm$ .003	0.772 $\pm$ .002	0.473 $\pm$ .013	3.196 $\pm$ .010	9.724 $\pm$ .082
DEMoGEN-MLD [66]	0.490 $\pm$ .003	0.680 $\pm$ .004	0.776 $\pm$ .003	0.288 $\pm$ .005	3.124 $\pm$ .011	9.785 $\pm$ .115
MotionDiffuse [72]	0.491 $\pm$ .001	0.681 $\pm$ .001	0.782 $\pm$ .001	0.630 $\pm$ .001	3.113 $\pm$ .001	9.410 $\pm$ .049
MotionDiffuse [72] $^{\S}$	0.523 $\pm$ .002	0.714 $\pm$ .004	0.807 $\pm$ .002	0.287 $\pm$ .005	2.912 $\pm$ .010	9.456 $\pm$ .107
DEMoGEN-MotionDiffuse [72] $^{\S}$	0.527 $\pm$ .002	0.719 $\pm$ .003	0.820 $\pm$ .004	0.141 $\pm$ .006	2.908 $\pm$ .009	9.628 $\pm$ .096

Table 13. **Quantitative results on the HumanML3D test set.**  $\S$  indicates that we train MotionDiffuse using an  $x_0$ -prediction objective and apply DDIM for inference.

---

**Prompt:**

I have a text description of a human motion. Your task is to split this description into exactly two separate sentences.

Each sentence should describe one distinct human motion. If the original text contains style, emotion, speed, or environment information, you must preserve it in the corresponding sentences. No additional information should be added if it is absent in the original text.

Focus on accurately capturing the original meaning. The two sentences, when combined as sequential or simultaneous motions, should reproduce the meaning of the original description.

**STRICT OUTPUT FORMAT** (must follow exactly):

- Return ONLY the two sentences joined by a single “#”.
- Both `<sentence1>` and `<sentence2>` must be non-empty and contain meaningful words (not just spaces or punctuation).
- No labels, no explanations, no numbering, no quotes, no code fences, no extra spaces, and do not repeat the input.
- The output must match the pattern: `<sentence1>#<sentence2>`

Example:

Input: a person is walking forward while waving his left hand.

Output: a person is walking forward#a person is waving his left hand.

Now split the following sentence:

---

Table 14. **Prompt for splitting human motion descriptions into two distinct sentences.**